Novel Side-Chain Liquid Crystalline Polyester Architecture for Reversible Optical Storage

Søren Hvilsted,*,† Fulvio Andruzzi,‡ Christian Kulinna,§ Heinz W. Siesler,§ and P. S. Ramanujam[||]

Department of Solid State Physics, Risø National Laboratory, DK-4000 Roskilde, Denmark, Centro Studi Processi Ionici di Polimerizzazione, Dipartimento di Ingegneria Chimica, Facoltà di Ingegneria, CNR, Via Diotisalvi 2, I-56100 Pisa, Italy, Department of Physical Chemistry, University of Essen, D-45117 Essen, Germany, and Optics and Fluid Dynamics Department, Risø National Laboratory, DK-4000 Roskilde, Denmark

Received February 11, 1994; Revised Manuscript Received November 29, 1994[⊗]

ABSTRACT: New side-chain liquid crystalline polyesters have been prepared by melt transesterification of diphenyl tetradecanedioate and a series of mesogenic 2-[ω-[4-[(4-cyanophenyl)azo]phenoxy]alkyl]-1,3-propanediols, where the alkyl spacer is hexa-, octa-, and decamethylene in turn. The polyesters have molecular masses in the range 5000–89 000. Solution ^{13}C NMR spectroscopy has been employed to identify carbons of polyester repeat units and of both types of end groups. Polyester phases and phase transitions have been investigated in detail by polarizing optical microscopy and differential scanning calorimetry for the hexamethylene spacer architecture with different molecular masses. Using FTIR polarization spectroscopy, the segmental orientation in unoriented polyester films induced by argon ion laser irradiation has been followed and an irradiation-dependent order parameter for the cyanoazobenzene mesogens calculated. FTIR is also utilized to follow the temperature-dependent erasure of the induced orientation. Optical storage properties of thin unoriented polyester films are examined through measurements of polarization anisotropy and holography. A resolution of over 5000 lines/mm and diffraction efficiencies of about 40% have been achieved. Lifetimes greater than 30 months for information stored have been obtained, even though the glass transition temperatures are about 20 °C. Complete erasure of the information can be obtained by heating the films to about 80 °C, and the films can be reused many times without fatigue.

1. Introduction

Side-chain liquid crystalline (SCLC) polymers have received increasing attention during the last decade due to their intriguing properties and a broad range of potential applications especially in the field of optics and optoelectronics.[1–12] A leading motivation is the unique possibility of combining the functionality of conventional low molar mass liquid crystals with the properties of macromolecules. This is mainly possible due to the linking of the different mesogenic groups to the polymer main chain through flexible alkyl spacers of varying length. It has been demonstrated that photoinduced orientation of dye-containing liquid crystalline polymers can be used for reversible optical data storage.[2,3,5,7,12] Their characteristic attributes include the requirement of very low recording powers, the possibility of complete erasure of information, very long storage times, high resolution, and high efficiency. Many write–erase cycles have been accomplished with these materials with little or no fatigue. A special and rapidly expanding class of SCLC polymers have pendant azobenzenes.[13] Frequently, the cyanoazobenzene mesogen has been introduced and investigated in SCLC homo- or copolymers based on polyacrylates[1,3,6–11] and polymethacrylates,[5] polystyrene and poly(α-methylstyrene),[14] polyesters,[2,6,15–17] and polysulfones.[18]

The SCLC polyesters are particularly interesting because their polyester nature intrinsically offers extended flexibility in main-chain tailoring due to possible interchange of both the acidic and the glycol part, both of which, in turn, can provide the linking site for the mesogen. So far, however, the cyanoazobenzene mesogen has only been linked to a malonate unit of a SCLC polyester.[2,6,15–17] Recently, we have developed an efficient procedure leading to a variety of mechanically attractive nonmesogenic side-chain polyesters based on 2-octadecyl-1,3-propanediol and diphenyl esters.[19–22] 2-Octadecyl-1,3-propanediol[20] and 2-substituted 1,3-propanediols with mesogenic groups different from the cyanoazobenzene[17,23] are initially based on the proper alkylation of diethyl malonate followed by reduction to the diol. We have recently elaborated the chemistry for the introduction of the cyanoazobenzene mesogen in particular, but easily extendable to other substituents as well, into the alkyl group of the 2-substituted 1,3-propanediols and thus considerably expanded the molecular design possibilities of SCLC polyesters for reversible optical storage.[24] One advantage of this particular architecture is its modular construction; the four parameters involved, viz., the length of the acidic part of the main chain, the length of the flexible side-chain spacers, the substituents on the azobenzene, and the molar mass, can be varied individually. This allows a systematic study of the influence of the four parameters on the optical storage properties. We have shown that all four of these parameters have significant influence on optical storage properties. Our preliminary results on reversible optical storage in SCLC polyesters based on tetradecanedioate show that permanent reversible storage in these polyesters can be obtained at high resolution.[25] A variation of the main-chain spacer length to the much shorter adipate shows an interesting biphotonic character.[26,27] The influence of the length of side-chain spacers and the effect of crystallinity have been presented recently.[28] The influence of the different

* To whom correspondence should be addressed.
† Department of Solid State Physics, Risø National Laboratory.
‡ CNR.
§ University of Essen.
|| Optics and Fluid Dynamics Department, Risø National Laboratory.
⊗ Abstract published in *Advance ACS Abstracts,* February 15, 1995.

0024-9297/95/2228-2172$09.00/0

substituents on the azobenzene has also been examined by us.[29]

In this work, we discuss in detail the preparation and characterization of this series of new SCLC polyesters. We also examine the photoinduced anisotropies in thin films of these polyesters. Photoinduced orientational behavior has been determined through Fourier transform infrared (FTIR) dichroism[9,11,30] and optical dichroism.[31] We employ FTIR spectroscopy with polarized radiation to evaluate the orientation of several side-chain liquid crystalline (SCLC) polyesters as a function of irradiation time. We demonstrate that in favorable cases the orientational behavior of the mesogenic groups, the spacer, and the main chain may be selectively monitored by focusing on specific absorption bands of the individual structural units. We shall also show that the response of the SCLC polyesters to visible laser irradiation depends on the length of the flexible spacer. Optical dichroic measurements have also been employed here to complement the FTIR studies. Whereas the FTIR studies are used mainly to determine the orientation of the mesogens, the optical dichroic measurements indicate the orientational behavior of the segments that are responsible for refractive index variation. Finally holographic measurements have been made on these films in order to demonstrate their potential in reversible optical storage.

2. Experimental Section

2.1. Syntheses. Preparation of Precursor and Monomers. The dicarboxylic acid precursor, diphenyl tetradecanedioate, was prepared and purified as described previously.[19] The new mesogenic 2-[ω-[4-[(4-cyanophenyl)azo]-phenoxy]alkyl]-1,3-propanediols were synthesized and purified as very recently described.[24,25] The partly deuterated 2-[10-[4-[(4-cyanophenyl)azo]-2,3,5,6-tetradeuterophenoxy]decyl]-1,3-propanediol was prepared starting from hexadeuterophenol.

Polyester Preparation. A typical polyester preparation is exemplified with the procedure for poly [2-[6-[4-[(4-cyanophenyl)azo]phenoxy]hexyl]-1,3-propylenetetradecanedioate] (P6a12-1). A mixture of 0.5333 g (1.398 mmol) of diphenyl tetradecanedioate and 0.5740 g (1.398 mmol) of 2-[6-[4-[(4-cyanophenyl)azo]phenoxy]hexyl]-1,3-propanediol was weighed into an approximate 10 mL spherical glass reactor, melted in a N_2 atmosphere, and homogenized by stirring achieved by rotating the reactor. After cooling to room temperature, 10 mg (5 mol % catalyst) of K_2CO_3 was added to the mixture and reheated to 120−130 °C under N_2 and reduced pressure (1300 Pa or 10 mbar) as long as sublimed phenol could be detected. Normally this phase took between 1 and 2 h. Then the temperature was slowly raised to 170 °C and the vacuum lowered down to 60 Pa or 0.5 mbar, and these conditions were maintained for 2 h. The polyester was recovered from the reactor after cooling by dissolution in 10 mL of benzene. The polyester solution was centrifuged and precipitated in 100 mL of methanol. The precipitated polyester was collected by filtration, air-dried, redissolved in 10 mL of benzene, centrifuged, and finally reprecipitated in 100 mL of methanol. After filtration the polyester was dried in a vacuum oven at room temperature for 16 h and 0.839 g (almost a 100% yield) was recovered.

2.2. Instrumentation. Intrinsic Viscosity. Limiting viscosity numbers of polyesters were measured in tetrahydrofuran at 303.15 K in an Ubbelohde viscometer.

Size-Exclusion Chromatography (SEC). Polyester SEC measurements were performed with a Knauer HPLC pump FR-30 fitted with a Rheodyne 7010 sample injection valve, typically equipped with a 100-μL loop, a 5-cm G 7000 Guard, and a 60-cm GMH mixed gel column (7.5 mm i.d.) from Toya Soda, Japan. Detection was accomplished with a Knauer high-temperature differential refractometer. Concentrations of polyesters were nominally 1% (w/v) in a stabilized tetrahydrofuran (technical grade) eluent at a nominal flow of 1 mL/min verified by a syphon counter. Investigations were performed either at 30 °C in a thermostatically controlled oven or at ambient temperature. Absolute weight-average molecular masses were investigated by low-angle laser light scattering (LALLS) with a Chromatix KMX-6 photometer coupled to an Optilab 5902 refractometer employing a light source operating at 632.8 nm and a Knauer HPLC pump. The necessary (dn/dc) determinations were performed on a 30-cm G1000H Toya Soda column on 3 mL 0.15% and lower (w/v) tetrahydrofuran solutions at a flow rate of 1.0 mL/min.

UV−Visible Absorption Spectroscopy. A Pye Unicam SP8-400 spectrometer was employed to record UV−visible spectra of the polyesters as an 0.04 mg/mL chloroform solution.

^{13}C Nuclear Magnetic Resonance (NMR) Spectroscopy. ^{13}C NMR spectra were recorded at 62.896 MHz on a Bruker AC 250 spectrometer. The spectra were obtained in 5-mm-i.d. tubes on 10−15% (w/v) solutions in $CDCl_3$ at 300 K. Spectra were recorded with a pulse width of 2.3 μs (≈45°); a 0.92-s pulse acquisition and a 2-s pulse repetition were used to obtain at least 2000 scans. Chemical shifts are referenced to the central resonance of $CDCl_3$ (76.90 ppm from tetramethylsilane).

Differential Scanning Calorimetry (DSC). DSC experiments were performed on a Perkin-Elmer DSC 4 instrument equipped with an Intracooler-I apparatus.

Polarizing Optical Microscopy (POM). The POM observations were made with a Leitz Ortholux-Pol BK polarizing microscope by use of a Mettler FP-52 hot stage controlled by a Mettler FP-5 unit.

Fourier Transform Infrared (FTIR) Polarization Spectroscopy. Thin films of the polyesters for FTIR investigations were obtained by casting a chloroform solution (2 mg of polymer in 200 μL) of each sample onto KBr plates with a 25-mm diameter. After evaporation of the solvent, the films were further dried at room temperature for 2 h under vacuum. The film thickness obtained by this preparation procedure was approximately 5 μm.

FTIR polarization spectra were recorded on a Perkin-Elmer 1760X spectrometer with a resolution of 4 cm^{-1} and a total of 32 scans. Polarization of the IR beam was obtained using a wire-grid polarizer with ZnSe as the substrate. The samples were mounted in the spectrometer in such a way that the polarization direction of the incoming IR beam was parallel to the polarization direction of the employed argon ion laser beam. By rotating the polarizer, the spectra were recorded with light polarized parallel and perpendicular to the polarization direction of the argon ion laser.

Temperature-dependent measurements were carried out in a heating cell mounted in the sample compartment of a Bruker IFS 88 spectrometer. Spectra were recorded at a resolution of 4 cm^{-1} and a total of 20 scans. Starting from 304 K, the temperature was increased at a rate of 1 K min^{-1} to a final temperature of 373 K and polarization spectra were taken with radiation polarized alternately parallel and perpendicular to the argon ion laser beam polarization direction previously used for irradiation of the sample. The temperature was controlled by a thermocouple fixed inside the KBr plates which were used as sample support. For the irradiation experiments, the 488 nm line of an argon ion laser was used. The intensity level of the argon ion laser was approximately 300 mW/cm^2, and the irradiated sample area was 20 mm^2. Irradiation time varied between 1 and 1000 s and was controlled by an automatic shutter.

Optical Anisotropy and Holographic Measurements. Optical and holographic measurements were performed on polyester films cast from a solution of 2 mg of polyester in 200 μL of chloroform onto optical glass plates, 5 cm in diameter. Before casting, the plates were thoroughly cleaned in a detergent solution, rinsed with distilled water, and dried. When the solvent had evaporated, the transmission loss at a wavelength of 633 nm was measured to be on the order of 50%, for a film thickness of approximately 5 μm. The films are not preoriented in any fashion.

A Spectra-Physics Model 2020 argon ion laser was employed for the irradiation experiments, normally at 488 nm. The readout was achieved with a 3-mW HeNe laser.

3. Results and Discussion

3.1. Syntheses and Characterization of the Polyesters. 3.1.1. Polyester Preparation. The stringent requirement for the stoichiometric equivalence in order to obtain product polyesters of high molecular mass is met by accurate measurement of carefully purified reactants. In the first step of the polymerization sequence a hydroxypropylene ester and phenol are formed:

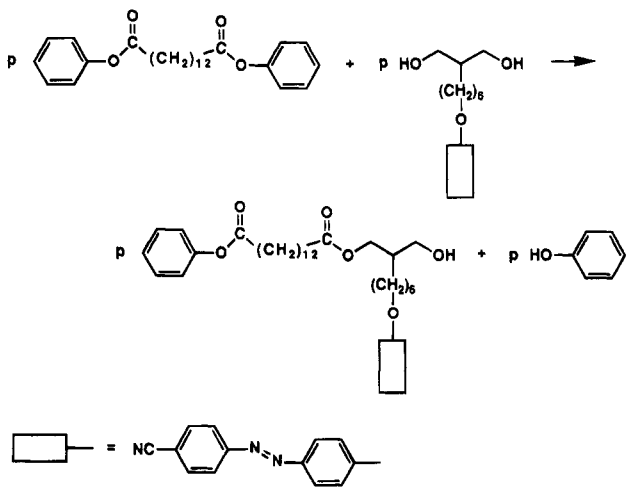

This step is intrinsically reversible, but the continuous removal of the volatile phenol will, under the adopted experimental conditions, drive the reaction in the outlined direction. During the second stage, the temperature was slowly raised to 170 °C and the vacuum lowered down to 60 Pa or 0.5 mbar in order to complete the ester exchange reaction and force the hydroxypropylene ester toward the polycondensation by alcoholysis, thus forming the polyester and liberating further phenol due to the chain growth process:

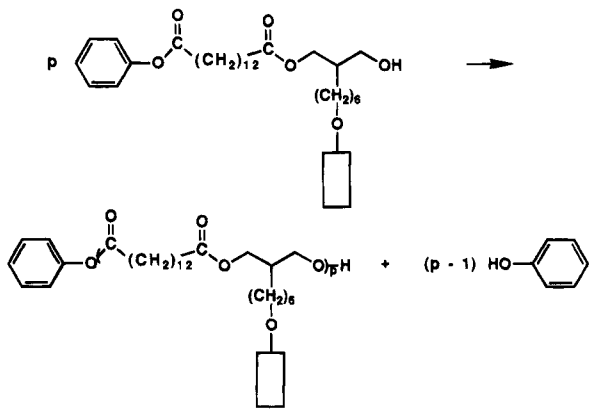

The choice of the final working temperature for the second stage was governed by the thermal stability of the azo group of the mesogenic units which starts to decompose at approximately 200 °C.[24] Also the duration of this second stage has a vital influence on the achievable molecular mass and mass distributions. The viscosity of the reaction mixture increased markedly with the conversion. The conversion can, in fact, be monitored continuously by determining the amount of evolved phenol by disconnecting the reactor and weighing. The polymerization process was continued until the polycondensation degree had reached the desired value, typically in the range $p \approx 10-100$; this corresponds to intrinsic viscosity numbers, $[\eta]$, of 0.1–0.9 dL/g in tetrahydrofuran at 30 °C. The necessary reaction time was generally on the order of 3–4 h.

Table 1. Intrinsic Viscosities and Molecular Masses of SCLC Poly(tetradecanedioates)

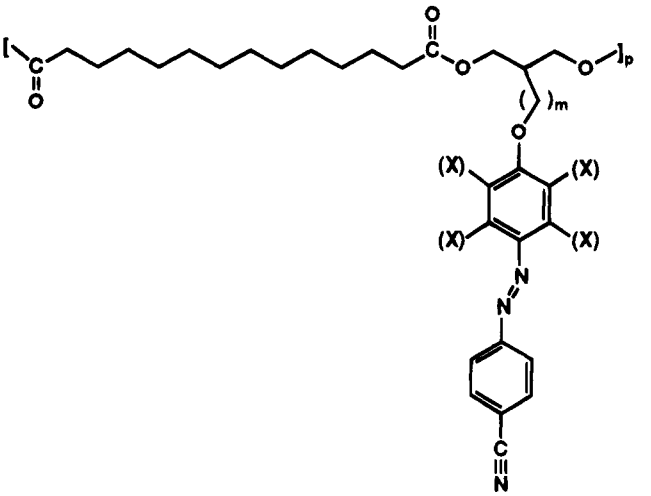

polyester	m	X	$[\eta]$ (dL/g)	M_p[a]	M_w[b]
P6a12-1	6	H	0.73	58 000	
P6a12-3	6	H	0.10	4 700	5 000
P8a12	8	H	1.01	89 000	
P10a12	10	H	0.94	68 000	
P10ad$_4$12	10	D	0.26	21 000	29 000

[a] From SEC peak position by use of a universal calibration with PS standards. [b] Determined by LALLS.

3.1.2. Polyester Characterization. The polyesters were characterized by intrinsic viscosity numbers and size-exclusion chromatography (SEC) with tetrahydrofuran as the solvent. Table 1, in addition to intrinsic viscosities and molecular masses, also indicates the structural differences of the SCLC poly(tetradecanedioates), change in length of flexible spacer (m), and different isotopic substitution (X) on the phenoxy moiety. The listed peak molecular masses (M_p) were calculated from the maximum position of the SEC distributions by use of a calibration curve constructed from polystyrene standards with narrow molecular mass distributions. The highest molecular masses, 58 000–89 000, of each representative polyester architecture are higher than molecular masses previously reported[15,17] on azobenzene containing SCLC polyesters being on the order of 14 000–56 000. The SEC characterizations of the three samples with $[\eta] = 0.73$ dL/g or above all revealed under careful inspection molecular mass distributions typical for condensation polymerization at high conversions, however, with broad shoulders on the high molecular mass side of the distributions. In fact, this observation was supported by findings from the attempted determination of the weight-average molecular mass (M_w) by use of low-angle laser light scattering (LALLS) coupled in series with the conventional refractive index (RI) detection. These experiments resulted in a dominating scattering signal corresponding only to the shoulder in the mass signal represented by the RI response. The data treatment of these experiments gave unrealistic high values which are not reported here. We believe that, although the thermogravimetric analyses[24] showed a thermal stability of the diol mono-

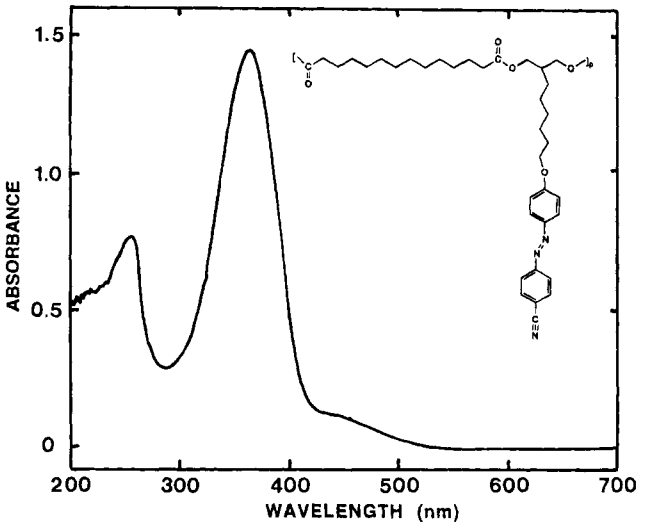

Figure 1. UV–visible absorption spectrum of P6a12-1 in chloroform.

mers up to 200 °C during the dynamic test (heating rate 1 °C/min), very little degradation taking place as a result of the extended time at the relatively high final temperature (170 °C) or local periodic overheating of already condensed diols could lead to phenyl radicals in the side chain. Two such radicals are then expected to recombine, and an effective branch would result. The dominating scattering signal is thus interpreted as resulting from branched polyesters. The other samples with lower $[\eta]$ values prepared by a slightly lower final temperature (160 °C), very careful temperature control, and shorter time showed symmetrically shaped SEC distributions of a somewhat narrower distribution. In these cases, no problems arose in the determination of M_w of these samples.

In addition to information on molecular masses and mass distributions, detailed insight into the polyester structure appears to be extremely important for the understanding of the physical phenomena resulting from the laser illumination and leading to the permanent refractive index modulations. Consequently, the prepared SCLC polyesters were additionally characterized with three spectroscopic techniques, UV–visible (Figure 1), ^{13}C nuclear magnetic resonance (NMR), and Fourier transform infrared (FTIR), each providing different structural information. In fact, the use of polarized FTIR, which, in addition, provides some polyester segmental information, is dealt with separately in a special section.

3.1.3. ^{13}C NMR Analyses. The principle information which can be obtained from ^{13}C NMR is illustrated with specific spectra of the high (P6a12-1) and the low molecular mass (P6a12-3) samples of P6a12. The ^{13}C NMR spectrum of P6a12-1 in a chloroform-*d* solution is shown in Figure 2 together with the polyester repeat unit. The labeled carbons of the repeat unit are unequivocally assigned by use of a combination of the detailed NMR information already existing on diphenyl tetradecanedioate,[19] aliphatic comb-shaped polyesters,[20] and 2-[6-[4-[(4-cyanophenyl)azo]phenoxy]hexyl]-1,3-propanediol.[24] The eight-methylene central segment of the dicarboxylic acid part and the two central methylenes of the flexible spacer are all collected in a complex multiplet, between 28.9 and 29.4 ppm, and cannot easily be resolved. The ^{13}C NMR spectrum of P6a12-3 in Figure 3, on the other hand, contains in addition to the resonances originating from the polyester repeat unit

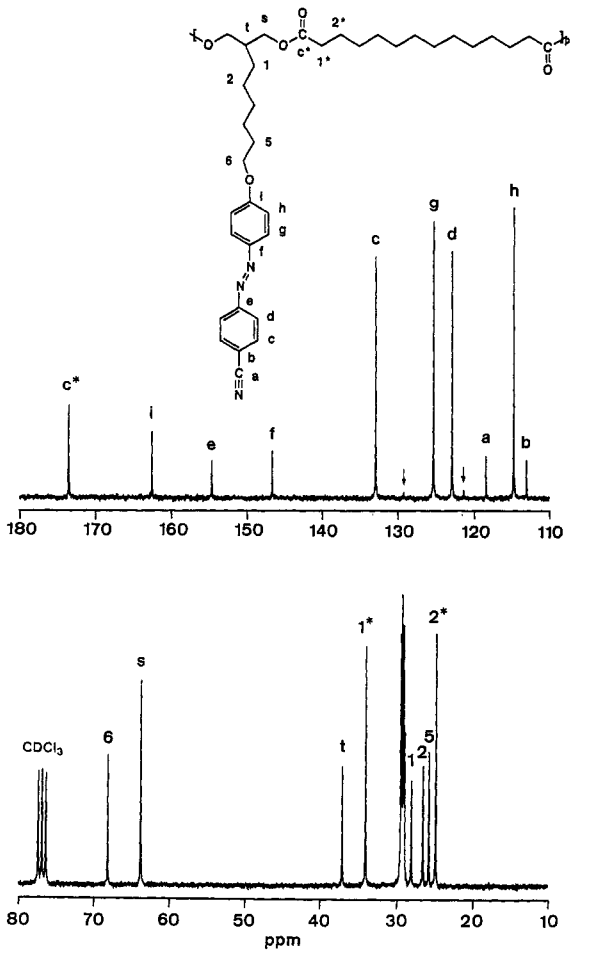

Figure 2. ^{13}C NMR spectrum of the polyester P6a12-1 in $CDCl_3$.

an abundance of other resonances. In fact, all the previously unresolved methylene resonances in both the main chain and spacer can be resolved in this case and assigned. The many new resonances in the carbonyl, aromatic, and aliphatic carbon regions of the spectrum either belong to actual end groups or are caused by the presence of such groups.

Three peaks in the aromatic region, at 129.37, 125.46, and 121.32 ppm, are the meta (m), para (p), and ortho (o) carbons, respectively, of a phenoxy moiety in a tetradecanedioate ester end group. The chemical shift values are exactly the same as found in the diphenyl tetradecanedioate.[19] Moreover, even the small peaks at 150.58 and 172.04 ppm arising from the quaternary (q) and the carbonyl (c_p*) of the phenyl tetradecanedioate can be observed. Even the first methylene group of the carboxylic part (1_p*) of an end-group appears to be slightly deshielded. From these findings, it is clear that the two minor peaks (↓) present in the spectrum of the high molecular mass polyester in Figure 2 stem from phenyl ester end groups. The existence of phenyl ester end groups in the side-chain polyesters prepared from diphenyl ester precursors has previously been identified[22] in an aromatic main-chain polyester of relatively low molecular mass and even in a sample with molecular mass more than 100 000.

The other possible end group, a 2-substituted 3-hydroxy-1-propylene ester, causes many new resonances. This situation has previously been modeled and discussed in detail for other polyesters based on similarly substituted diols.[32,33] The oxymethylene carbons (s in Figure 2) in an end group are nonsymmetric due to the

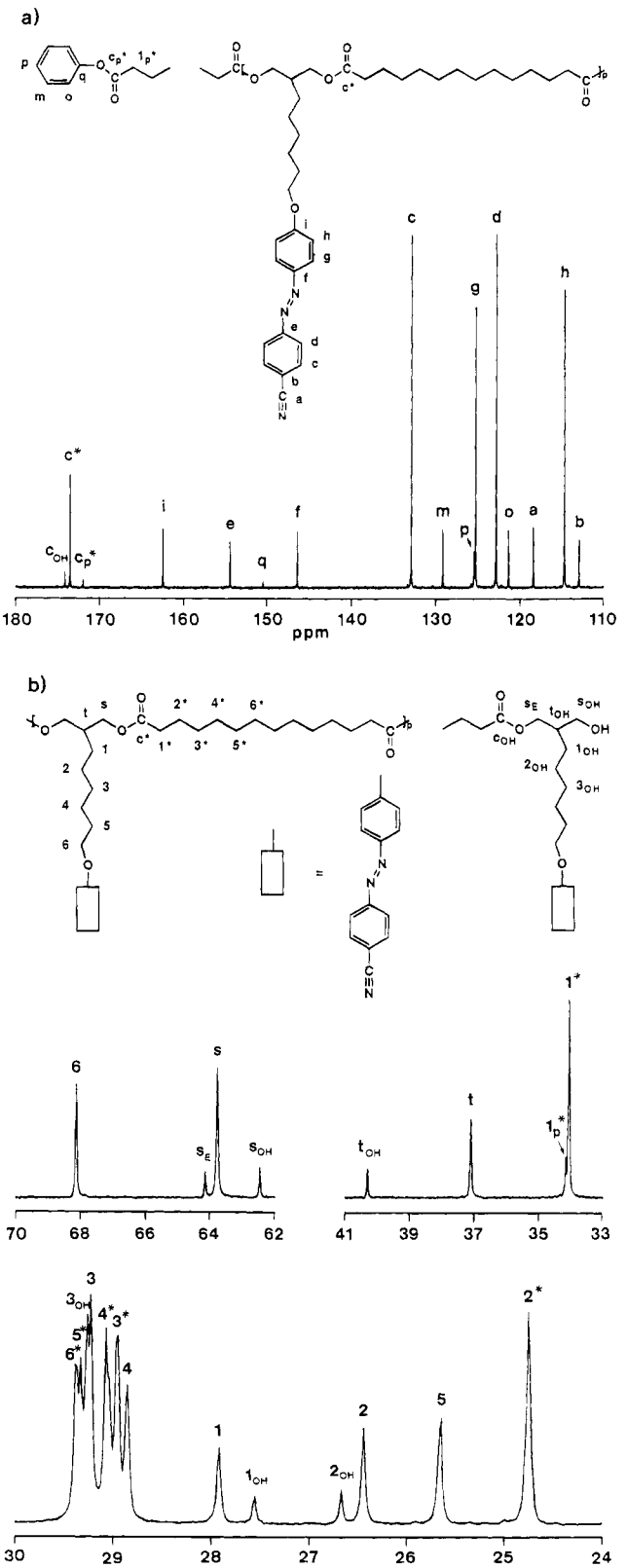

Figure 3. ^{13}C NMR spectrum of the polyester P6a12-3 in $CDCl_3$: (a) carbonyl and aromatic region; (b) aliphatic region.

different substitution. One of these carbons (s_E) becomes part of an ester group, as all the other in-chain s carbons in the polyester main chain, but was influenced also by the hydroxymethylene with a small deshielding as a result. The other carbon is the hydroxymethylene (s_{OH}) which is shielded compared to in-chain s carbons due to a combination of the different shielding behavior of hydroxyl and ester oxygen and the lack of especially one β-substituent. For the tertiary carbon (t_{OH}) in a 3-hydroxypropylene end group with one ester β-substituent and one hydroxyl β-substituent as compared to two β-ester substituents of the in-chain t carbons, an even larger deshielding (3.2 ppm) is observed. However, this effect is also in agreement with earlier observations[32,33] in other 3-hydroxypropylene ester end groups. In addition, also the two first methylene carbons of the flexible spacer of this end group, 1_{OH} and 2_{OH}, experience small shieldings and deshieldings, respectively, as compared to the situation prevailing in the in-chain units. It is furthermore indicated in Figure 3 that even the third methylene carbon of this end group (3_{OH}) possibly is slightly deshielded. This short 3-hydroxypropylene ester, in fact, also influences the carbonyl resonance (c_{OH}*) which is experienced to be (0.6 ppm) deshielded.

It should be added that these spectra are representative for the other polyesters as well, with the exceptions that the increase of the flexible spacer length also influences the complexity of the methylene multiplet and the implications arising from the deuterated phenoxy group of P10ad$_4$-12.

This rather detailed analysis of the displayed ^{13}C NMR spectra of both high and low molecular mass P6a12 has been presented in order to extract maximum possible structural information, and, in fact, all visible resonances have been assigned. Based on this, it is concluded that the low molecular mass polyester consists of linear main chains and the high molecular mass polyester predominantly is made of linear main chains since the postulated branching of the high molecular mass polyester is not extensive and is expected to be present at a level which is smaller than the detected end groups. It should be mentioned that the polyester work-up procecdure is expected to exclude any cyclic structures which the NMR analysis, of course, will not reveal. It can also be added that no evidence of cyclics could be detected from the SEC investigations.

3.1.4. Polarizing Optical Microscopy (POM). POM investigations were carried out in thin polyester films (4−6 μm thick) cast from chloroform solution. The polyester films were subjected to different thermal treatments with the primary aim of promoting formation and identification of optical textures typical of liquid crystal (LC) phases. It is important to note that for the high molar mass polyesters P6a12-1, P8a12, and P10a12 it was not possible to observe any specific LC textures except a recurrent and rather ill-defined grained texture lacking distinctive optical features, likely due to the high polymer viscosity. It is well established[34] that the high viscosity of the polymer melts can hinder the formation of well-identifiable LC textures. This is especially true for smectic polymers where the development of two-dimensional positional order promotes a further increase of viscosity. Accordingly, they often exhibit blurred textures consisting of fine granulated birefringent domains. Attempts to enlarge the fine grain textures of P6a12-1, P8a12, and P10a12 by annealing were unsuccessful. Therefore, POM observations were extended to low molar mass polyesters such as P6a12-3.

The textural pattern of a P6a12-3 film cooled from the isotropic state to room temperature, and its change on heating, is illustrated by the photomicrographs in parts a−d of Figure 4. An optical texture consisting of irregularly distributed fanlike areas and ellipsoids typical of the smectic A phase is shown in Figure 4a.

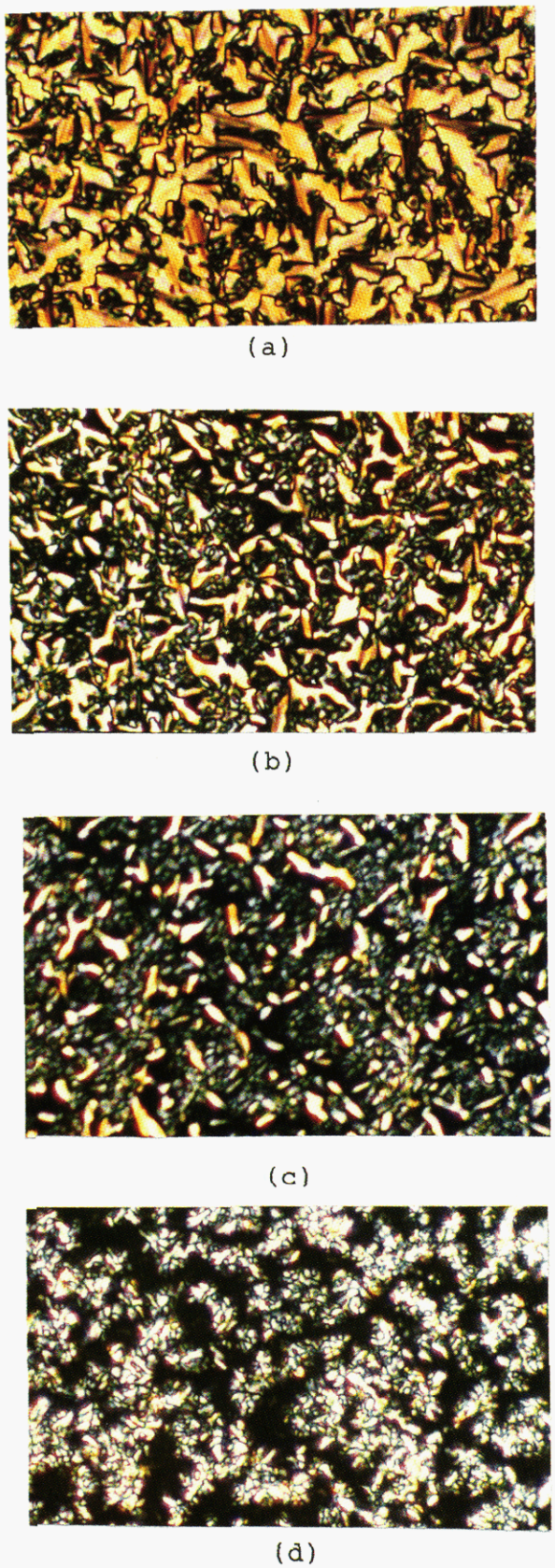

Figure 4. Photomicrographs showing optical texture changes, upon heating of a film of P6a12-3 cooled at 3 °C min^{-1} from 80 °C to room temperature: (a) 25, (b) 42, (c) 44, (d) 50 °C. Crossed polarizers. Magnification ×320.

Moreover, further inspection of the photomicrograph reveals the simultaneous presence of another optical texture. In order to examine the relevant pattern more in detail, the preparation was carefully heated in the microscope hot stage. The progressive attenuation, on

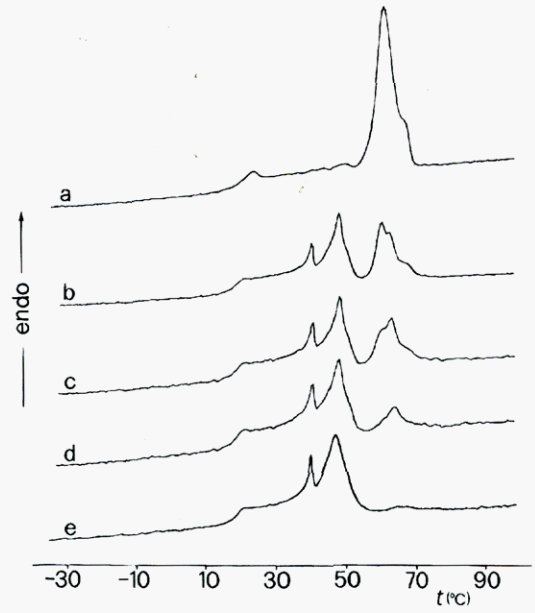

Figure 5. DSC heating curves of P6a12-3 polyester after cooling at different rates from the isotropic state: (a) 0.2, (b) 1, (c) 3, (d) 10, (e) 40 °C min^{-1}. Heating rate 3 °C min^{-1}.

heating, of smectic A birefringent texture is clearly observed in the photomicrographs in parts b and c of Figure 4. The texture disappears completely at about 50 °C (Figure 4d), thus allowing the identification of another, simultaneously present, optical texture consisting of floreate arrays of small birefringent grains, reminiscent of polycrystalline material. The birefringent scattered domains of this apparently crystalline phase disappear on further heating between 54 and 72 °C. Upon cooling at 3 °C min^{-1} the same texture is formed again, followed by the formation of elongated sharp-pointed particles (bâtonnets), thus indicating that the incoming smectic A mesophase of the polyester P6a12-3 is formed directly from the normal amorphous isotropic liquid. This provides further evidence about the coexistence of the two observed phases in the examined polyester preparation.

3.1.5. Polyester Characterization by Differential Scanning Calorimetry (DSC). The multiphase nature of polyester P6a12-3 was also confirmed by DSC measurements. Essential features of the thermal behavior of P6a12-3 samples after cooling at different rates are seen in the DSC traces in parts a–e of Figure 5. Inspection of the thermal traces in parts b–d of Figure 5 reveals in addition to the glass transition at ca. 19 °C, characteristic of the polyester backbone, two broad endotherms at 48 and 62 °C, pointing to a system substantially made by two independent phases. In agreement with the relevant POM observations, these endotherms have been assigned to first-order transitions from the smectic A LC state to the isotropic phase and from solid crystal to normal liquid, respectively. These assignments are consistent with the order of magnitude of the corresponding transition energies, ca. 7 and 16 kJ mol^{-1}, respectively. No specific assignment was possible for the small endothermic peak at 39 °C, which might be due to a hidden variant of polymorphism not observable by POM. From the comparison of the traces of Figure 5, it is clearly seen that the relative amount of the polyester crystalline phase is strongly dependent on the cooling rate. In particular, upon very slow cooling the polyester crystallization appears to reach the maximum extent, whereas the formation of the smectic

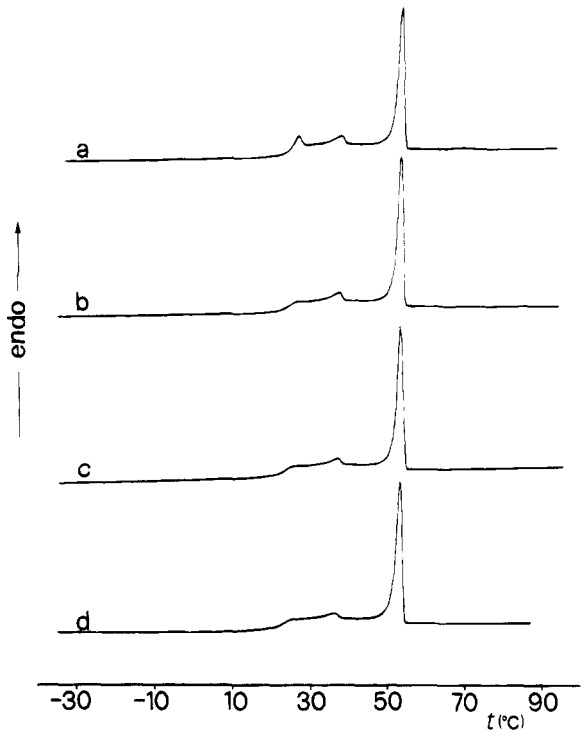

Figure 6. DSC heating curves of P6a12-1 polyester after cooling at different rates from the isotropic state: (a) 0.2, (b) 3, (c) 10, (d) 40 °C min^{-1}. Heating rate 3 °C min^{-1}.

phase is completely inhibited. Indeed, on reheating only the transition from the solid crystal to isotropic liquid is observed above T_g, as shown by DSC curve a of Figure 5. However, it is worth noting that for moderate and/or very low crystallinity degrees (curves b–e of Figure 5) the tendency of the polyester side chains toward smectic mesomorphism is effectively preserved. Under these conditions the low degree of polyester main-chain crystallinity apparently does not affect the anisotropically orientable mesogenic side groups.

The DSC traces of samples of the higher molar mass polyester P6a12-1, heat-treated in the same way as P6a12-3, are presented in Figure 6a–d. All the thermograms display, besides a glass transition at ca. 24 °C and a small endotherm at 36 °C, a sharp and intense endothermic peak at 54 °C. All the observed transitions are independent of the sample thermal treatment. Direct comparison of the DSC curves of Figure 6 with those of Figure 5 illustrates very clearly the strong effect on the polyester thermal behavior due to the increase of molar mass. The phase associated with the thermal transition at 54 °C is indicative of a poorly ordered smectic from results based on X-ray measurements. Anyway, in light of these results, it is difficult to explain the rather large enthalpy change observed for the above-mentioned thermal transition. Indeed, the observed enthalpy of 9.4 kJ mol^{-1} seems to be too large for a transition from a scarcely ordered smectic phase to the normal isotropic liquid. Transitions from or to a smectic B phase[35] can be on the order of 8 kJ mol^{-1}, but in this case the outer ring in the X-ray diffraction pattern is very sharp. Therefore, further characterization work is in progress to clarify this point.

3.2. Fourier Transform Infrared Polarization Spectroscopy Measurements. 3.2.1. Band Assignment and Orientation. Figure 7 shows one of the FTIR spectra with the molecular structure of the investigated SCLC polyester (P10a12).

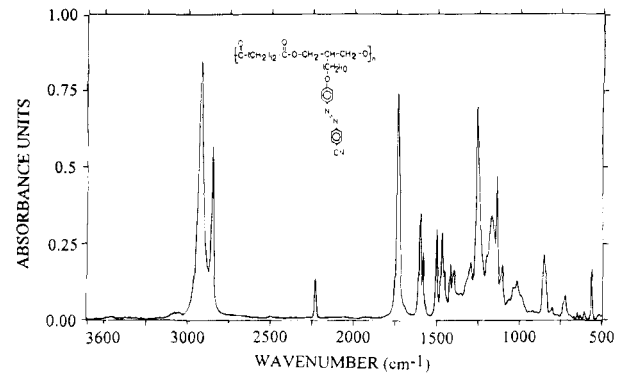

Figure 7. FTIR spectrum and molecular structure of the polyester P10a12.

Specific absorption bands can be assigned to the main chain, the spacer, and the mesogenic group. Characteristic absorptions of the mesogen are the aromatic ring modes (1601/1583 and 1501 cm^{-1}), the aromatic out-of-plane vibration (852 cm^{-1}), and particularly the isolated ν(C≡N) vibration at 2229 cm^{-1}. These absorption bands are useful probes for determining the orientation of the mesogens, whereas the orientational behavior of the main chain is reflected by the ν(C=O) absorption (1734 cm^{-1}) and various modes of coupled –COOR group vibrations (1200–1170 cm^{-1}). The doublet observed in the spectrum at 1471 and 1455 cm^{-1} can be assigned to the $\delta(CH_2)$ absorption bands of the methylene units in the main chain and the spacer, respectively. Band assignments were made with the aid of the monomers and monomer and polymer samples with deuterated aromatic rings, respectively.

3.2.2. Studies on Irradiated Films. Upon irradiation of the same sample with an argon ion laser, significant intensity differences can be detected in the corresponding spectra taken with IR radiation polarized parallel and perpendicular to the polarization plane of the argon ion laser beam, respectively. This photoinduced dichroism can be ascribed to a *trans–cis* photoisomerization of the azo group, followed by a *cis–trans* isomerization obtained by dark adaptation.[36,37] During these transitions the mesogens are able to orient themselves perpendicular to the electric field of the laser. This orientation remains after the "writing" beam has been turned off. In other words, a macroscopic orientation, which is stable for a long time, is generated.

From the dichroic behavior of the above-mentioned bands, it is possible to derive a model of the light-induced alignment. Here, the mesogenic side groups are oriented preferentially perpendicular to the polarization plane of the argon ion laser beam. This description is based on the σ-dichroism of the ν(C≡N) band (2229 cm^{-1}), the ν_{as}(C–O–C) band of the aromatic ether functionality (1254 cm^{-1}), and the absorptions of the aromatic ring modes (1601/1583 and 1501 cm^{-1}). Furthermore, this hypothesis is supported by the π-dichroism of the $\delta(C-H)_{ar}$ absorption (852 cm^{-1}). Figure 8 shows the development of the ν(C≡N) absorption band of the P10a12 polyester in these two directions as a function of increasing irradiation time from 1 to 1000 s. Figure 9 likewise demonstrates the total spectral changes for P10a12 after 100-s irradiation.

The alignment of the mesogenic part of the side chains should also induce an orientation of the methylene units in the spacer. The π-dichroism of the $\nu(CH_2)$ bands (2922 and 2852 cm^{-1}) can be interpreted in terms of an orientation of the methylene units in the spacer per-

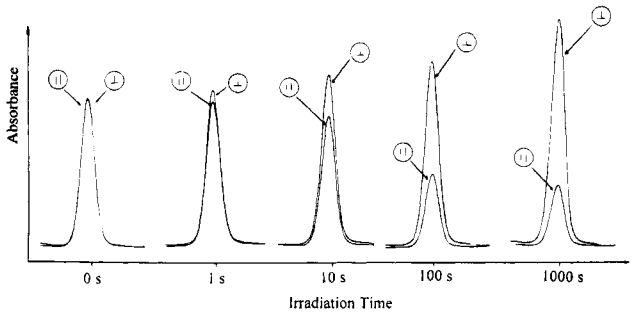

Figure 8. Irradiation time dependence of the ν(C≡N) vibration at 2229 cm^{-1} of the P10a12 polyester. IR beam polarized parallel (||) and perpendicular (⊥) to the plane of the applied argon ion laser beam (488 nm, 160 mW, ϕ = 5 mm).

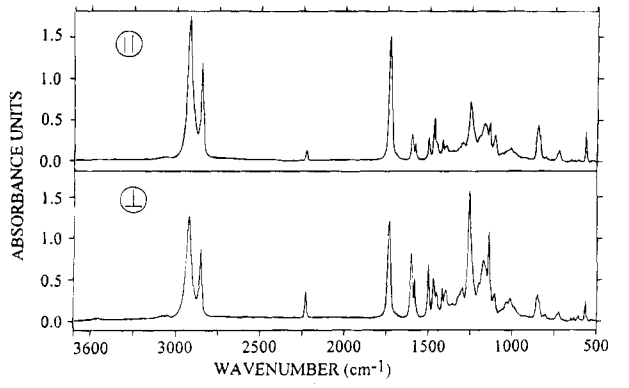

Figure 9. FTIR polarization spectra of irradiated P10a12. IR beam polarized parallel (||) and perpendicular (⊥) to the polarization of the argon ion laser beam (488 nm, irradiation 100 s, 160 mW, ϕ = 5 mm).

pendicular to the polarization of the argon ion laser beam. In the case of the PXa12 series, the order parameter (see below) evaluated from the dichroic ratio of the $\nu(CH_2)$ absorption bands increases by a factor of 2.6 on increasing the spacer length from 6 to 10 methylene units, while the number of methylene groups in the main chain is kept constant. This increase of the order parameter can also be observed by focusing on the CH_2 rocking vibration (720 cm^{-1}). This indicates that the dichroic behavior of these absorptions is influenced by the alignment of the spacer. The dichroic behavior observed for the doublet in the region of the $\nu(CH_2)$ vibrations (1471 and 1455 cm^{-1}) cannot be separately interpreted in terms of the orientation of the main chain and the side chains. A possible explanation is that this splitting is due to the *trans* and *gauche* conformation of the methylene units. A partially deuterated spacer or aliphatic dicarbonic acid will help to solve this assignment problem.

The orientation of the mesogens perpendicular to the plane of the argon ion laser polarization should also induce some kind of alignment in the main chain, since the mesogens and main chain are coupled via the methylene units of the spacer. This orientational effect is reflected in the dichroic behavior of the ν(C=O) absorption (1734 cm^{-1}). The π-dichroism of this band indicates a preferential alignment of the carbonyl groups in the direction of the laser beam polarization. The σ-dichroism of the ν(C−O−C) absorption of the ester (1172 cm^{-1}) confirms this conformational arrangement.

3.2.3. Determination of the Order Parameter. The orientation direction of the mesogenic groups is usually characterized by a unit vector, which is called the director. The director determines only the direction of the preferred orientation and indicates nothing about

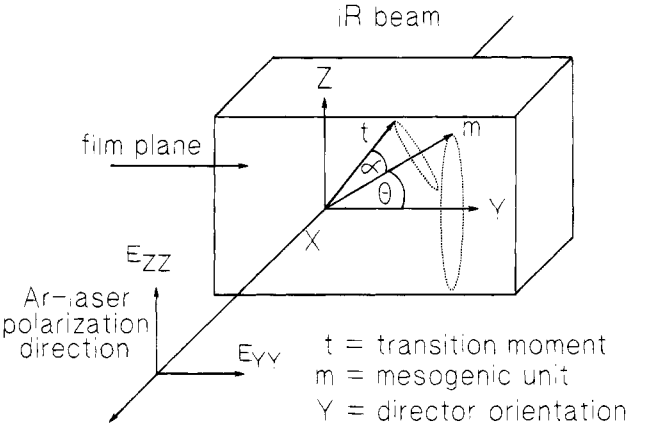

Figure 10. Geometry and experimental setup for the determination of the order parameter S_{yy}.

Table 2. Order Parameter (S) as a Function of Irradiation Time[a] for SCLC Poly(tetradecanedioates)

	irradiation time (s)				
polyester	0	1	10	100	1000
P6a12-1	0	0	0.02	0.12	0.5
P8a12	0	0.02	0.09	0.22	0.5
P10a12	0	0.03	0.14	0.61	0.7

[a] Irradiation at 488 nm with 160 mW.

the degree of orientational order in the mesophase. The order parameter S, introduced for low molecular mass nematic liquid crystals by Maier and Saupe,[38-40] provides just such a measure of the long-range orientational order. Thus, for our experimental conditions (see Figure 10) an order parameter S_{yy} can be defined:

$$S_{yy} = {}^1/_2\langle 3\cos^2\theta - 1\rangle \qquad (1)$$

where θ is the angle between the axis of the mesogenic segments and the director. Assuming a uniaxial distribution of the mesogenic units around the y-axis, the order parameter can be derived from infrared dichroism measurements by:

$$S_{yy} = [(R_0 + 2)(R - 1)]/[(R_0 - 1)(R + 2)] \qquad (2)$$

Here, R is the dichroic ratio (A_{yy}/A_{zz}) and R_0 is the dichroic ratio for perfect uniaxial alignment and is equal to 2 cot^2 α, where α is the angle between the transition moment direction and the mesogenic group axis. In the case of the ν(C≡N) vibration, $\alpha \approx 0°$ so that the expression simplifies to:

$$S_{yy} = (R - 1)/(R + 2) \qquad (3)$$

3.2.4. Order Parameter as a Function of Irradiation Time. For different SCLC polyesters, the order parameter has been evaluated as a function of irradiation time, using the dichroic effects of the ν(C≡N) absorption band. The samples vary in the length of the methylene units belonging to the spacer. The structural formula and the sample nomenclature is given in Table 1.

Table 2 gives an overview on the degree of orientation of the side chains in the different samples—indicated by the order parameter S—for different irradiation times. As can be seen from Table 2, the orientation of the side chains increases with irradiation time. It can also be seen that the alignment of the mesogenic groups increases with increasing spacer length. This can be

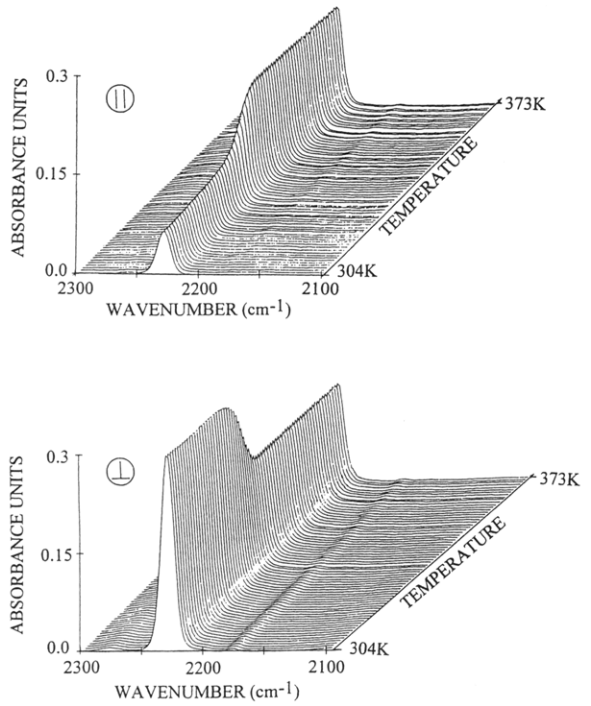

Figure 11. Temperature-dependent erasure of laser-induced orientation as demonstrated by the ν(C≡N) absorption band of the P10a12 polyester. IR beam polarized parallel (||) and perpendicular (⊥) to the polarization of the argon ion laser beam. Heating is performed from 304 to 373 K.

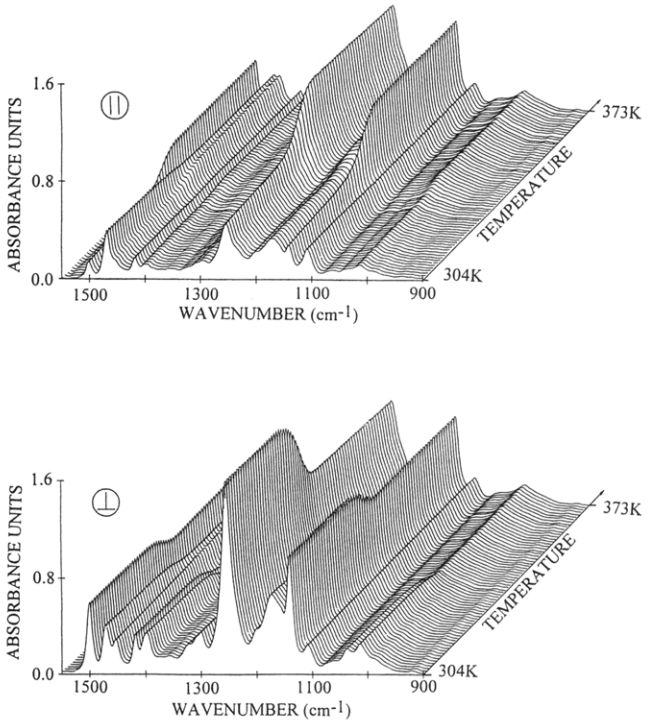

Figure 12. Temperature-dependent erasure of laser-induced orientation as demonstrated by the changes in the absorption intensities in the range from 1550 to 900 cm^{-1} of the P10a12 polyester. IR beam polarized parallel (||) and perpendicular (⊥) to the polarization of the argon ion laser beam. Heating is performed from 304 to 373 K.

explained in terms of their greater flexibility due to the spacer length. Furthermore, the response of samples to irradiation with long spacers is faster than that of short spacer samples. After an irradiation time of 10 s, for example, the sample with 10 and 8 methylene units in the spacer exhibits orientational effects which are respectively 7 and 4.5 times greater than that observed for the sample with the 6 methylene unit spacer. It is, however, expected that spacer length is not the only factor responsible for the magnitude of the order parameter although only small changes in side-chain length result in large changes in the orientational response to irradiation. For a more complete explanation of the observed effects, the phase behavior, mainly side-chain and main-chain crystallinity, and the occurring mesophases have to be taken into consideration.

3.2.5. Temperature-Dependent Measurements. The erasing and rewriting ability of the argon ion laser induced alignment in the SCLC polyesters is the basis for reversible optical data storage. To study this behavior, the induced orientation has been erased by heating the samples above their clearing temperature. This process has been followed by FTIR spectroscopy. Figure 11 shows the changes in absorption intensity of the ν(C≡N) band as a function of temperature for IR radiation polarized parallel and perpendicular to the argon ion laser polarization. From the spectra series shown, it can be seen that the alignment disappears around 341 K and the sample becomes isotropic. The loss of orientation can also be seen by focusing on the absorption bands of the aromatic ring stretching modes and the ν(C−O−C) absorptions (Figure 12) in the region 1550−900 cm^{-1}. Obviously, the disorganization process (even at this low heating rate) takes place in a narrow temperature interval and, therefore, the alignment is not sensitive to small temperature variations below the orientation−loss transition temperature.

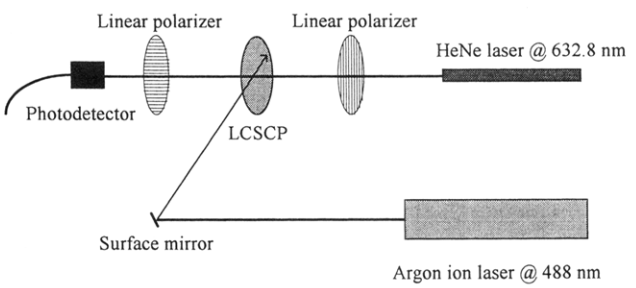

Figure 13. Experimental setup for the time-dependent measurement of the optical anisotropy in an LCSC polyester (LCSCP) film.

After erasing the orientation, it is possible to reproduce the alignment by further irradiation with the argon ion laser beam.

3.3. Optical Measurements. 3.3.1. Time-Dependent Measurement of Anisotropy. Figure 13 shows the experimental setup to measure the induced optical anisotropy as a function of time. The film is illuminated by a weak vertically polarized light from a HeNe laser at 633 nm. As seen from Figure 1, there should be no absorption in the film at this wavelength. An analyzer at 90° crosses out the light from the HeNe laser. A polarized argon ion laser beam at 488 nm with its polarization at 45° to the vertical is used to induce the optical anisotropy in the film. Measurements of the transmission will reveal the attainable refractive index difference due to the induced birefringence and also the photodynamics of the molecules. There is both photo-induced dichroism and anisotropy in the film, which are related through Kramers−Kronig relations. Figures 14−16 show the induced anisotropy for the polyester with 6, 8, and 10 methylene spacers as a function of time, for different intensities from the argon ion laser. The argon ion laser is switched off after 300 s, and the

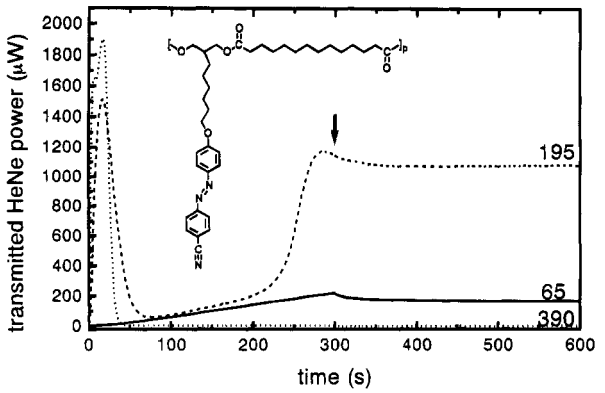

Figure 14. Optical anisotropy in an approximately 5-μm-thick film of P6a12-1 as a function of time for 65, 195, and 390 mW/cm^2 of the 488-nm argon ion laser line. The arrow indicates when the argon ion laser was switched off.

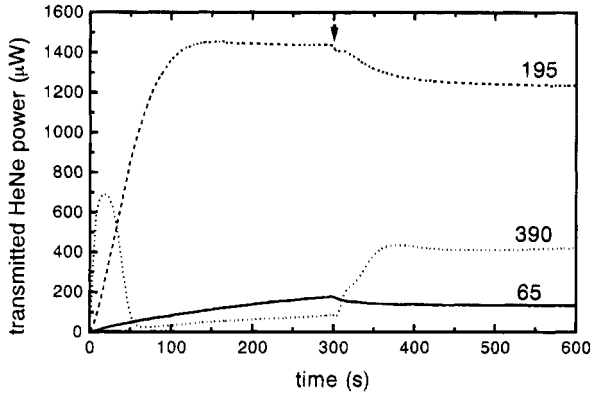

Figure 15. Optical anisotropy in an approximately 5-μm-thick film of P8a12 as a function of time for 65, 195, and 390 mW/cm^2 of the 488-nm argon ion laser line. The arrow indicates when the argon ion laser was switched off.

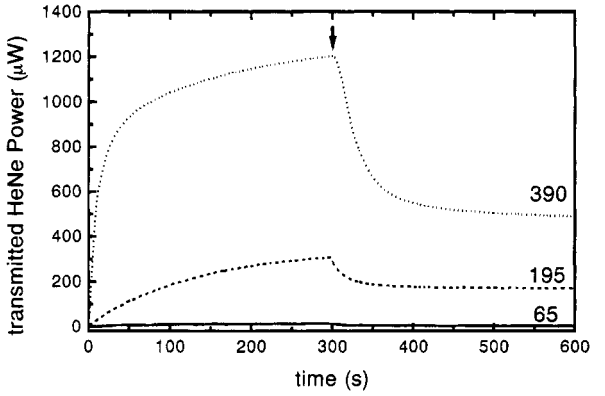

Figure 16. Optical anisotropy in an approximately 5-μm-thick film of P10a12 as a function of time for 65, 195, and 390 mW/cm^2 of the 488-nm argon ion laser line. The arrow indicates when the argon ion laser was switched off.

transmission is followed for 300 s more. For low intensities, on the order of 65 mW/cm^2, the transmission through the crossed polarizers increases, and after the argon ion laser is switched off, the transmission and thus the photoinduced anisotropy remain fairly constant. At 195 mW/cm^2, the film with 8 methylene spacers exhibits the largest response. A transmission of over 85% has been obtained for irradiation times larger than 200 s. The transmission of the film with the 10 methylene spacers has also increased, whereas that of the deuterated counterpart is found to be less. At 390 mW/cm^2, the polyester with 10 methylene spacers displays the largest transmission. It seems that

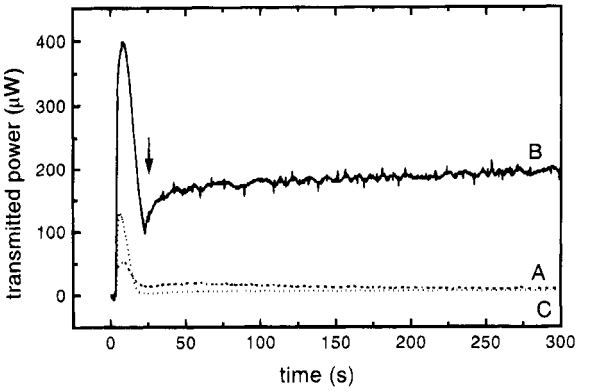

Figure 17. Optical anisotropy induced in a film of P6a12-1 by an argon ion laser beam at 488 nm with an intensity of 750 mW/cm^2 and probed at (A) 515, (B) 633, and (C) 780 nm. The arrow indicates when the argon ion laser was switched off after 25 s. The intensity of all probe beams was 30 mW/cm^2.

polyesters with shorter spacers respond more readily at lower intensities albeit with longer time constants. The polyesters with the longest spacers seem to possess a shorter time constant but also show a pronounced decay of the anisotropy after the laser is switched off. In most cases, a decrease in the transmission after reaching a maximum is observed for high laser intensities. The reason for the decrease is due to the phase difference caused by birefringence exceeding $\pi/2$.[28] In general, the light emerging from the film has been observed to be elliptically polarized. The experiment has been repeated at different probe wavelengths.

Figure 17 shows the anisotropy induced by an argon ion laser beam at 488 nm and probed at 515, 633, and 780 nm. The argon ion laser in this case is switched off after 30 s. The increased transmission at 633 nm is evident, the cause of which is still under investigation.

In order to understand the influence of molar mass on the storage properties, we have also studied the behavior of a low molar mass polyester. A comparison of the low molar mass polyester, P6a12-3, with that of high molar mass analogue, P6a12-1, shows that the response of the latter is much larger. This may be attributed to the difference in the length of the main chains. We believe that the higher molar mass exhibits a much higher cooperative motion of the main chain in response to the isomerization of the azo dye. We can also compare the transmission of the deuterated P10a12-d_4 with that of the undeuterated P10a12. The undeuterated sample shows a much higher response at all irradiated intensities than the deuterated one. The undeuterated sample has a larger molar mass basically due to the longer main chains. Assuming that the replacement of hydrogen with deuterium in the phenoxy ring does not have a profound significance, it can be concluded that the observed effect has the same origin as for the P6a12's, i.e., an increased cooperative motion of the main chain.

3.3.2. Holographic Measurements. A two-beam polarization holographic setup was used to record diffraction gratings. The absorption spectrum of an approximately 1-μm-thick film of P10a12 has previously been reported[25] and is very similar to the solution spectrum in Figure 1 from 300 to 700 nm. When examining the film in a polarization microscope at room temperature and using weak white light, the film exhibits no birefringence, and when performing conoscopic observations, no evidence of homeotropic align-

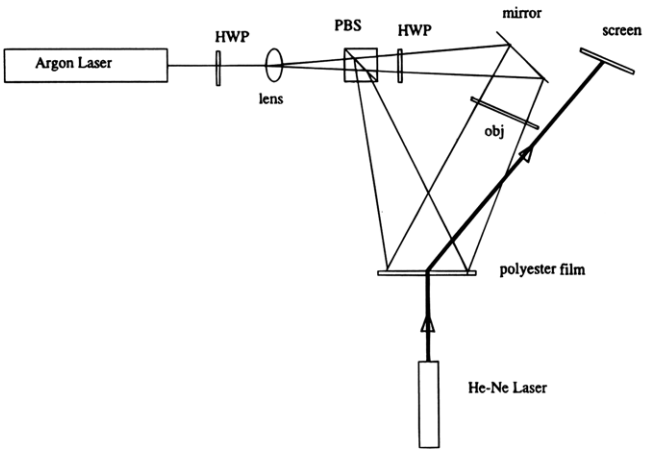

Figure 18. Setup for conventional two-beam polarization holography. HWP = half-wave plate; PBS = polarizing beam splitter.

ment of the mesogenic groups is seen. However, in most cases, a fine-grain texture characteristic for the presence of crystalline microdomains has been observed.

The setup for conventional two-beam polarization holography is shown in Figure 18. An argon ion laser beam at 488 nm is directed through a half-wave plate, to rotate the linearly polarized light from the laser, a lens, and further on to a polarizing beam splitter dividing the incident beam into two beams of equal intensity, and orthogonal polarizations. One of these beams is directed to the film, the second beam is directed by means of a mirror through an object, of which a hologram is desired, further on to the polyester film. If the object is removed, the coherent beams overlap, creating an ordinary polarization grating. It is known[41] that a polarization grating is capable of increasing the diffraction efficiency. The intensity of the beams can be adjusted to be between 1 mW/cm^2 and 1 W/cm^2. After exposure, the illuminated film, when examined between crossed polarizers, exhibits birefringence. The formation of the hologram is monitored by directing a HeNe laser beam at 633 nm from the rear side. The maximum diffraction efficiencies obtained is on the order of 35%. Using Kogelnik's equation[42] for diffraction efficiency:

$$\eta = \sin^2(\pi \Delta n d/\lambda)$$

where η is the diffraction efficiency, Δn, refractive index modulation, d, the thickness of the film, and λ, the wavelength of the probe beam; the maximum refractive index modulation under these exposure conditions is estimated to be about 0.025. Resolutions of 5000 linepairs/mm are easily obtained in these films. By directing two counterpropagating beams through the films, interference filters have been fabricated, indicating a line density of about 6000 linepairs/mm.

Figure 19 shows a recent photograph of the grating structure recorded in P6a12-1 over 2 years ago. The grating is viewed through crossed polarizers in a polarizing microscope. No sign of decay after a period of over 30 months is evident. Holograms have been recorded with all the visible wavelengths of the argon ion laser, i.e., between 455 and 515 nm. The holograms can be completely erased by heating the film above 80 °C, also demonstrated by the FTIR measurements presented in section 3.2.5. So far no fatigue has been measured even after several repeated cycles of recording and erasure.

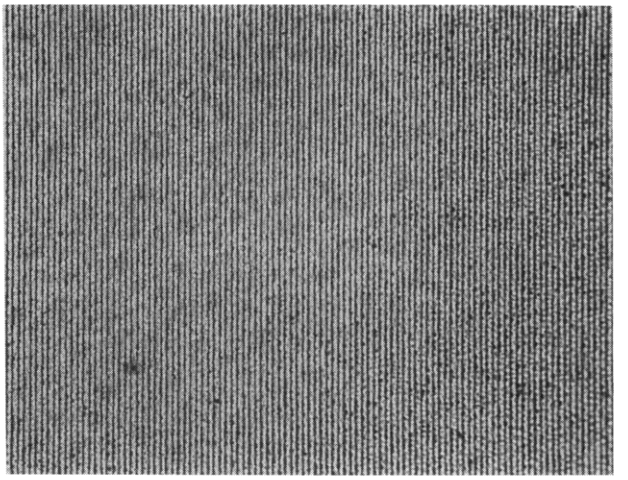

Figure 19. 1300 lines/mm grating structure recorded more than 30 month ago. Viewed through crossed polarizers in a polarizing microscope. Magnification ×400.

It has been pointed out by several authors[43,44] that a linearly polarized pump light beam orients the azochromophores perpendicular to the pump beam polarization direction, through cycles of photoisomerization. The reorientation process is caused by *trans* to *cis* transitions and *cis* to *trans* optical and thermal back transitions. This is also confirmed through FTIR spectroscopy. It is known from previous studies that even short illuminations of an absorbing dye film can increase the temperature of the film to greater than 200 °C for short periods of time.[45,46] This temperature is well above the glass temperature of the polyester, as a result of which the main and side chains acquire an increased mobility. The movement of the side chains, in all probability, induces a reorientation of the main chains as is also indicated by FTIR measurements. The alignment of the main chain is frozen once the incident light is removed, resulting in a permanent birefringence.

It has often been quoted in the literature that, in order to achieve a permanent recording, the glass temperature must be as high as possible.[43] However, our experiments show that, in spite of the fact that the glass temperature is as low as 24 °C in our polyesters, a long-lived storage has been achieved. We suspect that crystallization in the polyesters may have a strong role to play in the permanent storage of information.

The influence of the temperature of the film and the effect of the power of the argon laser are being studied in detail.

4. Conclusions

The preparation of azobenzene containing SCLC polyesters of a new molecular architecture and with relatively good control of the achievable molecular masses in the 5000−89 000 range is demonstrated. The light-induced orientational behavior of the azo polymers shows that the investigated materials comply with the requirements for reversible optical data storage. No prealignment of the samples has been found to be necessary. The orientation of the liquid crystalline side chains perpendicular to the polarization of the writing beam is achieved by the laser beam itself. Small changes in the number of methylene units in the side-chain spacer seem to result in large changes in the light-induced orientational behavior. This offers the possibility of tailoring the polymer for specific applications.

Moreover, it has been shown that FTIR polarization spectroscopy is a useful tool for the quantitative deter-

mination of the order parameter and the derivation of a model for the light-induced alignment of the molecules by focusing on specific absorption bands. In addition, FTIR spectroscopy can be used to follow the temperature-dependent erasure of the induced orientation.

Optical measurements of the polarization anisotropy induced by the argon ion laser corroborate the FTIR measurements. It is found that SCLC polyesters with longer side chains respond more readily to light irradiation, although at higher intensities. The HeNe laser beam at 633 nm is shown to have a strong influence on the alignment of the side chains, when the film is in an isotropic state. Holographic storage has been performed in thin films of these polyesters. A storage density of over 5000 lines/mm, corresponding to an eventual bit size of about 100 nm, a high diffraction efficiency of about 40%, and long storage lifetimes (greater than 30 months), has been achieved in these films. The information is completely erasable by heating the film to about 80 °C, and the film can be reused several times without fatiuge.

Acknowledgment. We express our thanks to Anne-Lise Gudmundsson (Roskilde University, Denmark) for recording the NMR spectra and to Lotte Hansen (Risø National Laboratory) for performing the SEC experiments. C.K. and H.W.S. (University of Essen, Germany) acknowledge the instrumental and financial assistance of Deutsche Forschungsgemeinschaft (Germany) and Fonds der Chemischen Industrie (Germany).

References and Notes

(1) Ringsdorf, H.; Schmidt, H.-W. *Makromol. Chem.* **1984**, *185*, 1327.
(2) Eich, M.; Wendorff, J. H.; Reck, B.; Ringsdorf, H. *Makromol. Chem., Rapid Commun.* **1987**, *8*, 59.
(3) Eich, M.; Wendorff, J. H. *Makromol. Chem., Rapid Commun.* **1987**, *8*, 467.
(4) McArdle, C. B., Ed. *Side Chain Liquid Crystal Polymers*; Blackie and Sons Ltd.: Glasgow, U.K., 1989.
(5) Anderle, K.; Birenheide, R.; Eich, M.; Wendorff, J. H. *Makromol. Chem., Rapid Commun.* **1989**, *10*, 477.
(6) Eich, M.; Wendorff, J. H. *Opt. Soc. Am. B* **1990**, *7*, 1428.
(7) Wiesner, U.; Antonietti, M.; Boeffel, C.; Spiess, H. W. *Makromol. Chem.* **1990**, *191*, 2133.
(8) Ivanov, S.; Yakovlev, I.; Kostromin, S.; Shibaev, V.; Läsker, L.; Stumpe, J.; Kreysig, D. *Makromol. Chem., Rapid Commun.* **1991**, *12*, 709.
(9) Wiesner, U.; Reynolds, N.; Boeffel, C.; Spiess, H. W. *Makromol. Chem., Rapid Commun.* **1991**, *12*, 457.
(10) Anderle, K.; Birenheide, R.; Werner, M. J. A.; Wendorff, J. H. *Liq. Cryst.* **1991**, *9*, 691.
(11) Wiesner, U.; Reynolds, N.; Boeffel, C.; Spiess, H. W. *Liq. Cryst.* **1992**, *11*, 251.
(12) Stumpe, J.; Muller, L.; Kreysig, D. *Makromol. Chem., Rapid Commun.* **1991**, *12*, 81.
(13) Xie, S.; Natansohn, A.; Rochon, P. *Chem. Mater.* **1993**, *5*, 403.
(14) Crivello, J. V.; Deptolla, M.; Ringsdorf, H. *Liq. Cryst.* **1988**, *3*, 235.
(15) Reck, B.; Ringsdorf, H. *Makromol. Chem., Rapid Commun.* **1985**, *6*, 291.
(16) Engel, M.; Hisgen, B.; Keller, R.; Kreuder, W.; Reck, B.; Ringsdorf, H.; Schmidt, H.-W.; Tschirner, P. *Pure Appl. Chem.* **1985**, *57*, 1009.
(17) Reck, B.; Ringsdorf, H. *Liq. Cryst.* **1990**, *8*, 247.
(18) Braun, D.; Herr, R.-P.; Arnold, N. *Makromol. Chem., Rapid Commun.* **1987**, *8*, 359.
(19) Hvilsted, S.; Andruzzi, F.; Cerrai, P.; Tricoli, M. *Polymer* **1991**, *32*, 127.
(20) Andruzzi, F.; Hvilsted, S. *Polymer* **1991**, *32*, 2294.
(21) Hvilsted, S.; Andruzzi, F.; Paci, M. *Polym. Bull.* **1991**, *26*, 23.
(22) Andruzzi, F.; Hvilsted, S.; Paci, M. *Polymer* **1994**, *20*, 4449.
(23) McRoberts, A. M.; Denman, R.; Gray, G. W.; Scrowston, R. M. *Makromol. Chem., Rapid Commun.* **1990**, *11*, 617.
(24) Hvilsted, S.; Andruzzi, F. Manuscript in preparation.
(25) Hvilsted, S.; Andruzzi, F.; Ramanujam, P. S. *Opt. Lett.* **1992**, *17*, 1234.
(26) Ramanujam, P. S.; Hvilsted, S.; Andruzzi, F. *Appl. Phys. Lett.* **1993**, *62*, 1041.
(27) Ramanujam, P. S.; Hvilsted, S.; Andruzzi, F.; Kulinna, C.; Siesler, H. W. In *Organic Thin Films for Photonic Applications*; Technical Digest Series Vol. 17; Optical Society of America: Washington, DC, 1993; p 244.
(28) Ramanujam, P. S.; Hvilsted, S.; Andruzzi, F. *Opt. Rev.* **1994**, *1*, 30.
(29) Zebger, I.; Kulinna, C.; Siesler, H. W.; Andruzzi, F.; Pedersen, M.; Ramanujam, P. S.; Hvilsted, S. *Macromol. Symp.*, submitted.
(30) Bräuchler, M.; Boeffel, C.; Spiess, H. W. *Makromol. Chem.* **1991**, *192*, 1153.
(31) Rochon, P.; Gosselin, J.; Natansohn, A.; Xie, S. *Appl. Phys. Lett.* **1992**, *60*, 4.
(32) Hvilsted, S. In *Organic Coatings, Science and Technology*; Parfitt, G. D., Patsis, A. V., Eds.; Marcel Dekker: New York, 1986; Vol. 8, pp 79–108.
(33) Hvilsted, S. In *Biological and Synthetic Polymer Networks*; Kramer, O., Ed.; Elsevier Applied Science Publishers: England, 1988; Chapter 15, pp 243–254.
(34) Donald, A. M.; Windle, A. H. *Liquid Crystalline Polymers*; Cambridge University Press: Cambridge, U.K., 1992; Chapter 5, p 159.
(35) Gray, G. W.; Goodbye, J. W. G. *Smectic Liquid Crystals*; Leonard Hill: Glasgow and London, 1984; Chapter 2, p 43.
(36) Eisenbach, C. D. *Photogr. Sci. Eng.* **1979**, *23*, 183.
(37) Jones, C.; Day, S. *Nature* **1991**, *351*, 15.
(38) Maier, W.; Saupe, A. *Z. Naturforsch.* **1959**, *14a*, 882.
(39) Maier, W.; Saupe, A. *Z. Naturforsch.* **1961**, *16a*, 816.
(40) Wedel, H.; Haase, W. *Ber. Bunsen-Ges. Phys. Chem.* **1976**, *80*, 1342.
(41) Todorov, T.; Nikolova, L.; Tomova, N. *Appl. Opt.* **1984**, *23*, 4309.
(42) Kogelnik, H. *Bell. Syst. Technol. J.* **1969**, *48*, 2909.
(43) Natansohn, A.; Rochon, P.; Gosselin, J.; Xie, S. *Macromolecules* **1992**, *25*, 2268.
(44) Haitjema, H. J.; von Morgen, G. L.; Tan, Y. Y.; Challa, G. *Macromolecules* **1994**, *27*, 6201.
(45) Bartholomeusz, B. J. *Appl. Opt.* **1992**, *31*, 909.
(46) Evans, K. E. *J. Appl. Phys.* **1988**, *63*, 4946.

MA9450290